

# Survey of land cover datasets for updating the imperviousness field in urban parameterisation scheme TERRA\_URB for climate and weather applications



Carmela Apreda<sup>a,\*</sup>, Jan-Peter Schulz<sup>b</sup>, Alfredo Reder<sup>a</sup>, Paola Mercogliano<sup>a</sup>

<sup>a</sup> Fondazione Centro Euro-Mediterraneo sui Cambiamenti Climatici, Regional Models and Geo-Hydrological Impacts (REMHII) Division, Via Thomas Alva Edison, 81100 Caserta, Italy

<sup>b</sup> Deutscher Wetterdienst (German Meteorological Service), Research and Development, Frankfurter Str. 135, 63067 Offenbach am Main, Germany

## ARTICLE INFO

### Keywords:

Land cover  
Impervious surface area  
Urban climate modelling  
Urban canopy parameters

## ABSTRACT

In climate modelling, a critical issue is the accurate representation of urban areas in space and variation over time. Urban features may be parameterised through urban canopy parameters (UCPs), including the impervious surface area (ISA). One of the aims of the Consortium for Small-scale Modelling (COSMO) and the CLM-Community is to improve urban numerical weather prediction (NWP) and climate simulations by implementing the urban canopy scheme TERRA\_URB in the ICOSahedral Nonhydrostatic (ICON) modelling framework. To harmonise and update the datasets adopted for the UCPs, the Consortium has launched the Priority Project “City Induced Temperature change Through A’dvanced modelling” (PP CITTA). Within this framework, the study explores recent and detailed land cover datasets to update ISA and harmonise it with datasets adopted for the UCPs. We identify and compare some relevant datasets at the pan-European level. The results show the benefits obtained by correlating the UCPs from urban Local Climate Zones taken from the ECOCLIMAP-Second Generation with the ISA depending on the imperviousness degree provided by the Copernicus Land Monitoring Service. These results will foster an updating of NWP and climate models with urban surface parameterisations to match urban features while avoiding inconsistencies consistently.

## 1. Introduction

The land cover represents a key source of information for investigating morphological and functional changes occurring in terrestrial ecosystems and the environment, including climate change and the carbon cycle (Sleeter et al., 2018). Governments and scientific communities use this information to understand and observe changes related to human activities, coordinate climate change mitigation and adaptation actions, improve forest management, and monitor agricultural land availability (Tsendbazar et al., 2015). Land cover change may affect different ecosystem services, resulting in loss of biodiversity, disruption of the hydrological cycle, increase in soil erosion, microclimatic discomfort and runoff (IPCC, 2022).

Land cover plays an essential role in influencing climate patterns or weather events. The Global Climate Observing Systems has recognised land cover as one of the 19 terrestrial Essential Climate Variables due to its dynamics over time (e.g. seasons, years) and

\* Corresponding author.

E-mail address: [carmela.apreda@cmcc.it](mailto:carmela.apreda@cmcc.it) (C. Apreda).

variability on a spatial scale (e.g. global, regional, local) (GCOS, 2023). Moreover, several simulations have shown that the results of numerical models are sensitive to underlying changes in land cover (Shepherd et al., 2010; Davin et al., 2020), highlighting the need for proper land cover characterisation.

Several land cover maps are available for numerical models for weather prediction and climate projections. Unfortunately, most of them introduce these data exogenously, keeping them constant and neglecting the interaction between land cover change and climate variations (Lin et al., 2013). This approximation is expected to be particularly relevant in climate applications.

In order to consider this interaction, several studies tried to understand the effect of land cover change on climate processes, but limited studies accounted for its dynamic nature (Bukovsky et al., 2021; Zhang et al., 2021). The impact of time-varying land cover data in numerical models is currently investigated in a joint community effort, i.e. the Land Use and Climate Across Scales Flagship Pilot Study (LUCAS FPS) supported by the World Climate Research Program-Coordinated Regional Climate Downscaling Experiment (WCRP-CORDEX) and initiated by the European branch of CORDEX (EURO-CORDEX). In the first phase of LUCAS, idealised experiments at relatively low resolution (50 km) are performed to gain insights into the biogeophysical role of forests across a range of European climates. Future phases of LUCAS will focus on historical and future land cover changes and the added value of higher (kilometre-scale) resolution when assessing local land cover change impacts (Davin et al., 2020).

Other relevance in considering both time variability and increased spatial is expected in the Convection-Permitting Regional Climate Models (CP-RCMs, Prein et al., 2015), which represent a promising tool enabling representation of the land surface at scales of <4 km. They enhance the simulation of localised precipitation features and those factors activating convection, such as interactions with complex topography, urban effects, land-ocean contrasts, and land surface heterogeneities (Ban et al., 2014; Berthou et al., 2018; Coppola et al., 2020; Fumière et al., 2020; Reder et al., 2020; Fosser et al., 2015; Prein et al., 2015; Piazza et al., 2019; Adinolfi et al., 2021; Raffa et al., 2021; Ban, 2021; Fowler et al., 2021; Reder et al., 2022). CP-RCMs may also support the study of complex and fine-scale aerosol-cloud-precipitation interactions, indirectly improving the representation of regional climate through various feedback mechanisms, such as soil moisture-precipitation and soil moisture/vegetation-temperature.

The development of CP-RCM often results in applications where a high number of grid points include urban areas, thus requiring numerical models to simulate urban climate dynamics. To accurately simulate the complex interplay between urban areas and their environment, a key priority is to find a better representation of land surface features involving urban areas, capturing the heterogeneity of the city's morphology and coverage, and their variation over time. These features may be described through a set of urban canopy parameters (UCPs), such as the building height, impervious/pervious fraction area (i.e., percentage of impervious surface area – ISA), aspect ratio of the street canyon and thermo-physical parameters (e.g. albedo, emissivity, heat capacity and thermal conductivity of urban materials). However, the quantification of these parameters is still a challenging issue.

One of the objectives of the Climate Limited-area Modelling Community (CLM-Community) and the Consortium for Small-scale Modelling (COSMO) is to develop and improve a regional atmospheric model for climate simulations and numerical weather prediction (NWP), respectively. Formerly, this was the COSMO-CLM model (Baldauf et al., 2011), which is now being replaced by the ICON (ICOahedral Non-hydrostatic, Zängl et al., 2015) model. ICON is a global atmospheric model that can also be applied in limited area mode for NWP and climate simulations. Based on the COSMO and ICON land surface scheme TERRA-ML (Schulz et al., 2016; Schulz and Vogel, 2020), the bulk urban canopy scheme TERRA\_URB (Wouters et al., 2017) was developed for both climate and weather applications. TERRA\_URB provides an intrinsic representation of urban physics by modifying input data (introducing external UCPs) and allowing for detailed simulations of urban land-atmospheric interactions. Furthermore, to describe the heterogeneity of the urban surface, it adopts a tile approach, whereby urbanised and natural parts can act simultaneously in each grid cell. Specifically, physical variables are simulated separately for urban and natural tiles (using TERRA\_URB and TERRA-ML equations, respectively) and then area-averaged according to the ISA, which defines the fraction of urban area in a cell. Currently, COSMO and ICON models adopt the GlobCover 2009 (Arino et al., 2009) dataset for land cover and, when TERRA\_URB is activated, datasets from the European Environmental Agency (Maucha et al., 2010) for ISA and Flanner (2009) for the anthropogenic heat flux, while the other external parameters are assumed as constant. However, the GlobCover 2009 still includes a land cover class identifying urban areas (i.e. land cover class 19). In this sense, it should be noted that ISA is not the same as the urban land cover area fraction. Specifically, ISA refers only to artificial areas that do not allow precipitation to infiltrate the ground, including a variety of surfaces related to i) structures, ii) mobility systems, and iii) other compacted and non-vegetated areas. Conversely, the urban area fraction represents the land use class 19 of GlobCover 2009, which comprises all artificial surfaces and associated areas (urban areas >50%). It could also include small green areas, such as gardens or parks.

As different datasets are considered for land cover and ISA, this urban land cover class may introduce inconsistencies and potential urban double-counting effects. On the one hand, it may be that a grid cell presents ISA = 0 and land cover class = 19: this appears as an inconsistency as the grid cell acts as 100% natural according to TERRA\_URB, even if its external parameters are calculated according to the urban land cover class. On the other hand, it may be that a grid cell presents ISA > 0 and land cover class = 19: this leads to counting the urban effects twice, once when adopting the urban scheme TERRA\_URB and otherwise when referring to natural tile external parameters, which take into account urban surfaces.

Potential strategies to reduce such inconsistencies and improve the accuracy and reliability of model results are to recalculate the affected external parameters, excluding the land cover class 19 of GlobCover and harmonising datasets used to define external UCPs due to the differences between the urban land cover class and the ISA parameter. In 2021, as part of the gradual transition from the COSMO to the ICON model, the COSMO Consortium launched the Priority Project “City Induced Temperature change Through Advanced modelling” (COSMO PP CITTÀ, <https://bit.ly/3H4qwAF>) whose ambition is to develop and implement these strategies.

The present work attempts to contribute to this topic by exploring the more recent and detailed land cover datasets developed specifically to provide information on impervious classes and different external UCPs. First, a desk review activity has selected existing

**Table 1**

Summary of the main characteristics of land cover datasets.

Dataset	Resolution		Coverage		Source of information (satellite data, external datasets)	Classification scheme	Thematic accuracy	Reference
	Spatial	Temporal	Spatial	Temporal				
<b>Land cover datasets with urban field</b>								
GlobCover	300 m	Single year	Global	2009	Medium Resolution Imaging Spectrometer Instrument Fine Resolution (MERIS FR) surface reflectance mosaics	FAO LCCS 22 classes	67,5%	ESA and UCLouvain, 2010
ESA CCI/C3S LC project	0.002778° (≈ 300 m)	Yearly	Global	1992–2020	MERIS Full and Reduced Resolution archive, Advanced Very-High-Resolution Radiometer, SPOT-Vegetation, PROBA-Vegetation and Sentinel-3 OLCI time series + Global Human Settlement Layer (GHSL) and Global Urban Footprint (GUF) for urban field	FAO LCCS 22 classes	70,5% (2020)	ESA-CCI, 2022
GLC2000 (Regional dataset)	0.00892857° (≈ 960 m)	Single year	European	2000	VEGA 2000 dataset (SPOT 4 satellite)	FAO LCCS 22 classes	n.a.	EU-JRC, 2003
CORINE Land Cover, CLC	100 m	Single year	European	1990–2000 - 2006 - 2012 - 2018	Sentinel-2, Landsat-8 (year 2018)	44 classes	≥ 85% (2018)	EEA, 2018
ECOClimap-SG	300 m	Single year	Global	2018	ESA-CCI global land cover map + CLC and GHSL for urban field	33 classes	n.a.	CNRM, 2018a
<i>Land cover datasets with ISA field</i>								
GAIA	30 m	Yearly	Global	From 1985 to 2018	Landsat data (Landsat Thematic Mapper - TM, Enhanced Thematic Mapper Plus - ETM+, Landsat 8 Operational Land Imager - OLI)	Non-impervious/impervious areas	≥ 90% (mean value for 1985, 1990, 1995, 2000, 2005, 2010, and 2015)	Gong et al., 2019
GAUD	30 m	Yearly	Global	From 1985 to 2015	Landsat data + GHSL, GUF, Global Urban Land, GAIA for urbanised land + the annual time series (1985–2015) of the Normalized Urban Areas Composite Index	Non-impervious/impervious areas	76% (2000–2015)	Huang, 2020
CLMS Imperviousness Density, IMD	100 m 20 m 10 m (2018)	Single year	European (EEA39)	2006–2009 - 2012 - 2015 - 2018	Sentinel-1, Sentinel-2	Degree of imperviousness (0–100%)	> 90% (urban areas, 2018)	EEA, 2020a

\* Single year datasets are developed for specific reference years.

land cover datasets at global and pan-European scales. Next, these datasets have been investigated by comparing their main characteristics (e.g. spatial and temporal coverage, spatial and temporal resolution, classification schemes) and identifying the land cover classes that best represent the ISA field. Once the most coherent datasets have been selected for integration and harmonisation purposes, a pan-European assessment has been performed to highlight the reliability of these datasets objectively. Such an assessment has been further deepened by examining the cities of Barcelona (Spain), Budapest (Hungary) and Milan (Italy), chosen as test cases representing heterogeneous urban contexts.

This paper shows the results of this evaluation and is structured as follows. First, Section 2 describes the results of the desk review activity, grouping land cover datasets into categories and highlighting shared features and differences. Then, Section 3 outlines the methodology developed to compare the different datasets. Finally, Section 4 presents and discusses the main results of the pan-European comparison, focusing on the local level for the three test cases.

## 2. Desk review of land cover datasets available for Europe

Land cover maps represent spatial information of different types (classes) of biophysical coverage (e.g., vegetated areas, artificial land, bare soil and wet areas and water bodies) observed on the Earth's surface (Di Gregorio and Jansen, 2000).

In general, land cover is often confused with land use, although land use does not describe the Earth's surface coverage but defines how people use the land to obtain products and benefits. Land use refers to the purpose the land serves, for example, recreation, wildlife habitat or agriculture, which could occur in a forest, grasslands or on manicured lawns. Land use may differ for lands with the same cover type (e.g. a land cover type of forest may be used for timber production or recreation, and it might be private land or a popular state park). The main difference is that land use indicates how people use the land, whereas land cover indicates the physical land type (Coffey, 2013).

Relevant information to determine land cover can be derived from different sources and inventory techniques (e.g. field surveys, aerial photography, satellite sensors). It may be possible to infer land cover from land use and vice versa, but often this relationship is not so evident due to the difficulty of observing land use (EEA, 2004).

Many global land cover mapping activities are now available. However, due to the vast diversity of dataset characteristics (e.g. information source, inventory techniques, classification scheme, sampling design, accuracy, etc.), it is necessary to consider and assess the suitability of the data for the specific application (Verburg et al., 2011).

This section presents the results of a desk review of land cover datasets currently available at the European scale (see Table 1). These datasets vary for spatial and temporal resolution, coverage, and classification schemes. According to the typology of provided information, they have been grouped into:

1) datasets providing information on all urban areas, artificial surfaces and associated areas resulting from human activities, including green urban areas and other unsealed surfaces (from now on, referred to as "Land cover datasets with URBAN field");

2) datasets providing information on impervious surfaces excluding all vegetated areas (from now on, referred to as "Land cover datasets with ISA field").

In the following, the datasets in Table 1 are described and compared according to spatial and temporal resolution, spatial and temporal coverage, classification scheme, and thematic accuracy.

### 2.1. Land cover datasets with URBAN field

The term "urban" generally refers to areas with a high percentage of artificial cover (e.g. 50–80%) due to human activities, including the built environment, transportation systems, infrastructure networks, extraction and waste disposal sites. It could also include small green areas, such as gardens or parks. Land cover datasets with urban classes are based on different classification systems and terminology. In this desk review activity, a pool of five datasets has been identified (see Table 1): GlobCover (ESA and UCLouvain, 2010), ESA CCI/C3S LC project (ESA-CCI, 2022), GLC2000 (EU-JRC, 2003), CORINE Land Cover (CLC, EEA, 2018), and ECOCLIMAP Second Generation (CNRM, 2018a). The datasets are generated by different satellite instruments and data and external datasets, as shown in Table 1.

The main difference between these datasets is the classification scheme for land cover classes. The most widely accepted classification is the FAO Land Cover Classification System (LCCS, Di Gregorio and Jansen, 2000). It is a hierarchical classification that identifies 22 land cover classes and satisfies global consistency and regional flexibility objectives by aggregating regionally defined legends into more generalised global LC classes (Bartholomé and Belward, 2005). GlobCover, GLC2000, and ESA-CCI/C3S LC projects rely on LCCS. These datasets contain two levels of land cover information: 1) a thematically detailed regional optimised land cover developed at continental and sub-continental levels; 2) a less thematically detailed global legend that harmonises regional legends into one consistent product (Bartholomé and Belward, 2005; Bontemps et al., 2011; Defourny et al., 2017). More in detail, they define urban areas as "*Artificial surfaces and associated areas*", i.e., areas with artificial cover resulting from human activities that greatly influence runoff and peak flow characteristics of water and the associated areas where the original surface is removed (e.g. extraction sites), or where materials have been deposited on top of the original surface (e.g. waste dumps and other types of deposit, Di Gregorio and Jansen, 2000).

The other land cover datasets with the URBAN field (i.e., CLC and ECOCLIMAP-SG) adopt a different classification scheme for land cover classes. CLC recognises 44 land cover classes grouped using a tree structure of a 3-level hierarchy. For example, urban areas are defined in level 1 (i.e., Artificial Surfaces), which is in turn subdivided into urban fabric; industrial, commercial and transport units; mine, dump and construction sites; artificial, non-agricultural vegetated areas (Kosztra et al., 2019). On the other side, ECOCLIMAP-SG

is based on the ESA-CCI global land cover map whose class “Urban areas” is identified using ancillary data (CLC2012 and Global Human Settlement Layer) that are reclassified and translated into multiple urban fields by adopting the ten urban Local Climate Zones (LCZs, [Stewart and Oke, 2012](#); [CNRM, 2018b](#)). LCZ refers to a classification system that comprises 17 classes at the local scale, 10 of which can be described as urban ([Table 2, Stewart and Oke, 2012](#)). Specifically, each LCZ represents a combination of surface structure, cover and human activity, providing baseline ranges for sky view factor, aspect ratio, building surface fraction, impervious and pervious surface fraction, the height of roughness elements, surface admittance, surface albedo, and anthropogenic heat flux (see [Tables 3 and 4 in Stewart and Oke, 2012](#)). In particular, LCZs define the impervious surface fraction as the proportion of ground surface with impervious cover (paved, rock), which affects surface reflectivity, moisture availability and heating/cooling potential, and is calculated as the ratio of impervious plan area (i.e., paved, rock) to total plan area ([Stewart, 2011](#); [Stewart and Oke, 2012](#)).

A further difference between these datasets is in their spatial resolution. Most datasets (i.e., GlobCover2009, ESA-CCI global map, and ECOCLIMAP-SG) feature a spatial resolution of 300 m. Conversely, GLC2000 is delivered at ~1 km spatial resolution, while CLC is at 100 m. Moreover, the datasets are mainly developed for specific reference years, except for the ESA-CCI/C3S LC project, which was provided from 1992 to 2020. In particular, CLC is one of the pan-European components of the Copernicus Land Monitoring Service (CLMS). It includes information on land cover for the reference years and its changes between two consecutive inventories across Europe ([Büttner et al., 2021](#)). The first land cover map was released in 1990, and updates were produced in 2000, 2006, 2012 and 2018. The variation in temporal resolution reveals the importance of dynamic datasets, such as the ESA-CCI global map, which include the evolution of land cover classes over time, capturing their change, while the static ones refer to a fixed dataset with no yearly updates. Another difference concerns the spatial coverage: GlobCover, ESA-CCI/C3S LC project and ECOCLIMAP-SG were developed as global products, while GLC2000 and CLC have European coverage.

Finally, the thematic accuracy is analysed regarding the quality of land cover products. Unfortunately, information on accuracy is not available for all datasets, e.g. ECOCLIMAP-SG and GLC2000, for which the operation is still in progress. Nevertheless, the overall accuracy of GlobCover reaches 67.5% using 2190 points globally distributed and including homogeneous and heterogeneous landscapes ([Bontemps et al., 2011](#)). The same for the ESA-CCI/C3S LC Project, evaluated on 1344 samples, is 70.5% ([Defourny et al., 2021](#)), while for CLC2018, it is higher than 85%. The quality of CLC products is also assessed considering the geometric accuracy, which is better than 100 m for 2018.

## 2.2. Land cover datasets with ISA field

ISA refers to artificial areas that do not allow precipitation to infiltrate the ground, resulting in surface runoff. It includes a variety of surfaces related to i) structures (e.g. buildings, roofs, sheds, decks, patios and large retaining walls); ii) mobility systems (e.g. roads, parking lots, sidewalks, driveways; iii) other compacted, non-vegetated areas. Three datasets have been identified in this desk review activity (see [Table 1](#)). They are the Global Artificial Impervious Area (GAIA; [Gong et al., 2020](#)), the Global Annual Urban Dynamics (GAUD; [Liu et al., 2020](#)), and the Copernicus Land Monitoring Service Imperviousness Density (CLMS-IMD; [EEA, 2020a](#)). These datasets, generated by different satellite instruments, data and external datasets ([Table 1](#)), share a similar classification scheme, with some differences, as described below.

First, they discern between impervious and pervious pixels without any information on the typology of land coverage. GAIA and GAUD adopt a binary code to identify impervious and pervious pixels, while CLMS-IMD also provides further details on the percentage of imperviousness density (0–100%). Moreover, GAIA and GAUD are long-term datasets to monitor the change of artificial impervious areas and urban dynamics worldwide. GAIA defines artificial impervious areas as “*mainly man-made structures that are composed of any material that impedes or prevents natural infiltration of water into the soil. They include roofs, paved surfaces, hardened grounds, and major road surfaces mainly found in human settlements*” ([Gong et al., 2020](#)). On the other hand, GAUD identifies urban areas as pixels dominated by built elements (e.g. buildings, roads, runways); it also defines the “urban expansion” as the increase in an urban area over time that occurs when non-urban covers are transformed into urban, and “green recovery” as built-up areas reverting to more vegetation-dominated states during the study period (e.g. reconstruction of parks or vegetation planting on built-up areas). Finally, CLMS-IMD defines the sealed/impervious areas replacing the original (semi-) natural land cover or water surface with an artificial and often impervious cover. It captures the spatial distribution of artificially sealed areas, including the level of soil sealing per area unit for a specific reference year.

All the datasets are developed with a very high spatial resolution, equal to 30 m for GAIA and GAUD and 100 m and 20 m (or 10 m for 2018) for CLMS-IMD. GAIA and GAUD are released as yearly products (1985–2018 and 1985–2015, respectively). On the contrary, CLMS-IMD is only available for five reference years (i.e., 2006, 2009, 2012, 2015 and 2018). Moreover, GAIA and GAUD are developed as global products, while CLMS-IMD has European coverage. Finally, regarding the thematic accuracy, GAIA data are evaluated for 1985, 1990, 1995, 2000, 2005, 2010, and 2015 using 2000 validation samples, and the mean overall accuracy is higher than 90% ([Gong et al., 2020](#)). The accuracy of mapped urbanised years for GAUD is assessed by selecting 140 major cities globally, and it is equal to 70% for the period 1985–2000 and 76% for the period 2000–2015 ([Liu et al., 2020](#)). The thematic accuracy assessment of CLMS-IMD 2018 is based on a sample set of 18,005 reference points. The overall accuracies exceeded the target of 90%, especially in urban areas. However, all these values are not sufficiently representative as the urban area makes up a relatively small fraction of the European landscape, even in the most densely built-up areas ([EEA, 2020b](#)).

## 3. Comparison of the land cover datasets

The review conducted in Section 2 highlights some differences among datasets. In particular, the land cover datasets with urban

**Table 2**

Definition of the ten urban LCZs provided by ECOCLIMAP-SG.

Dataset	Local Climate Zone (Urban type)	Definition (Stewart and Oke, 2012)
ECOCLIMAP-SG	24. LCZ1: Compact high-rise	Dense mix of tall buildings to tens of stories. Few or no trees. Land cover mostly paved. Concrete, steel, stone, and glass construction materials.
	25. LCZ2: Compact midrise	Dense mix of midrise buildings (3–9 stories). Few or no trees. Land cover mostly paved. Stone, brick, tile, and concrete construction materials.
	26. LCZ3: Compact low-rise	Dense mix of low-rise buildings (1–3 stories). Few or no trees. Land cover mostly paved. Stone, brick, tile, and concrete construction materials.
	27. LCZ4: Open high-rise	Open arrangement of tall buildings to tens of stories. Abundance of pervious land cover (low plants, scattered trees). Concrete, steel, stone, and glass construction materials.
	28. LCZ5: Open midrise	Open arrangement of midrise buildings (3–9 stories). Abundance of pervious land cover (low plants, scattered trees). Concrete, steel, stone, and glass construction materials.
	29. LCZ6: Open low-rise	Open arrangement of low-rise buildings (1–3 stories). Abundance of pervious land cover (low plants, scattered trees). Wood, brick, stone, tile, and concrete construction materials.
	30. LCZ7: Lightweight low-rise	Dense mix of single-story buildings. Few or no trees. Land cover mostly hard-packed. Lightweight construction materials (e.g., wood, thatch, corrugated metal)
	31. LCZ8: Large low-rise	Open arrangement of large low-rise buildings (1–3 stories). Few or no trees. Land cover mostly paved. Steel, concrete, metal, and stone construction materials
	32. LCZ9: Sparsely built	Sparse arrangement of small or medium-sized buildings in a natural setting. Abundance of pervious landcover (low plants, scattered trees).
	33. LCZ10: Heavy industry	Low-rise and midrise industrial structures (towers, tanks, stacks). Few or no trees. Land cover mostly paved or hard-packed. Metal, steel, and concrete construction materials

**Table 3**

Spatial correlation between LCZs provided by ECOCLIMAP-SG and ISA provided by GAIA 2018, GAUD 2015 and CLMS-IMD 2018 over Europe.

LCZs	ECOCLIMAP-SG	ISA					
		GAIA 2018		GAUD 2015		CLMS-IMD 2018	
		Pervious cells	Impervious cells	Pervious cells	Impervious cells	Pervious cells	Impervious cells
Natural LCZs	Natural LCZs	93,1%	1,6%	93,3%	1,7%	88,7%	6,4%
Urban LCZs	Urban LCZs	2,4%	2,9%	2,1%	2,9%	1,0%	3,9%

**Table 4**

Spatial correlation between LCZs provided by ECOCLIMAP-SG and ISA provided by CLMS-IMD 2018 at the local level.

LCZs	ECOCLIMAP-SG	CLMS-IMD 2018					
		Barcelona		Budapest		Milan	
		Pervious cells	Impervious cells	Pervious cells	Impervious cells	Pervious cells	Impervious cells
Natural LCZs	Natural LCZs	45%	11%	71%	8%	37%	17%
Urban LCZs	Urban LCZs	9%	35%	4%	18%	6%	40%

fields are based on classes, including green urban areas (e.g., gardens and parks) or built-up areas, without considering other sealed surfaces on the ground. Among these, ECOCLIMAP-SG seems to be the most promising. ECOCLIMAP-SG is a land cover dataset complemented by primary parameter fields (albedo, LAI, tree height and ground depths) and other parameters (including urban parameters associated with the ten urban LCZs) that are given through the SURFEX code (Le Moigne et al., 2018). The UCPs (e.g. building height, impervious fraction, etc.) are not explicitly provided by ECOCLIMAP-SG (CNRM, 2018a): a table with UCPs retrieved from SURFEX is associated to each LCZ that can be incorporated as input data in regional climate or NWP models with an urban parameterisation. In contrast, the datasets with the ISA field clearly distinguish between impervious and pervious pixels, albeit missing further details about the types of artificial areas.

In order to meet the goal of harmonising external UCPs and ISA and finding a spatial consistency between the datasets to associate LCZs with the ISA field, the selection of datasets considers both the presence of ISA values and the availability of additional parameters, such as the UCPs included in LCZs that could be adopted as external input for very high-resolution regional atmospheric models. For these reasons, not all land cover datasets with urban fields are suitable for this study. As shown in Fig. 1, the comparisons focus only on

the following datasets with LCZs and ISA values: 1) ECOCLIMAP-SG; 2) GAIA; 3) GAUD; 4) CLMS-IMD.

This section describes the two types of comparisons carried out in this study:

**C1.** The first comparison aims to identify datasets' reliability in representing ISA, capturing urban heterogeneity, the difference between land cover classes and the relationship between ISA and LCZs. GAIA, GAUD, CLMS-IMD and ECOCLIMAP-SG datasets are compared at the pan-European level by considering the most recent version available and the 300 m spatial resolution of ECOCLIMAP-SG.

**C2.** The second comparison aims at identifying a relationship between ISA and UCPs associated with the local climate zones. The survey concerns comparing the most reliable dataset for ISA among GAIA, GAUD, and CLMS-IMD (as brought out by the C1 comparison) to ECOCLIMAP-SG at the local level on a shared grid at 300 m.

The selection of cities for the comparison C2 takes into account some criteria to identify heterogeneous urban contexts, such as geographic location and historical and cultural background. The study areas are analysed considering the boundary of Functional Urban Area (FUA), which is defined as the area of the city plus its commuting zone. FUA consists of an area including a densely inhabited city and a less densely populated commuting zone whose labour market is highly integrated with the city (Dijkstra and Poelman, 2012)<sup>1</sup>. The present study compares land cover datasets by adopting the FUAs to include, in the boundary of each city, its surrounding area. The adoption of FUA, which is an official territorial typology defined by EUROSTAT, allows us to make further comparisons with other cities that could be included in future studies. The study areas are the following: Barcelona (ES), Budapest (HU) and Milan (IT).

### 3.1. Comparison at the pan-European level

In the first step, the urban fields provided by ECOCLIMAP-SG with the LCZs were compared with the ISA fields provided by GAIA, GAUD and CLMS-IMD at the pan-European level. Consistent to associate LCZs with the ISA field, the datasets have been compared by adopting the spatial resolution of ECOCLIMAP-SG. GAIA 2018 (30 m), GAUD 2015 (30 m), and CLMS-IMD 2018 (100 m) are aggregated onto the 300 m ECOCLIMAP-SG resolution.

Spatial correlation analysis among datasets has been carried out to identify the spatial relationship between the LCZs of ECOCLIMAP-SG and pervious/impervious cells of land cover maps with ISA field. The analysis identifies similar values that cluster together on the maps (positive spatial correlation) and contrasting values (negative spatial correlation), highlighting the need for further investigation to understand the reasons behind the spatial variations among the datasets.

The positive correlation is between: i) impervious cells and urban LCZs; ii) pervious cells and natural LCZs. Table 3 shows the spatial correlation between cells with natural/urban LCZs and pervious/impervious coverage. GAIA and GAUD show similar spatial correlation: the overall positive correlation over Europe is about 96%, of which only about 3% is associated with impervious cells and urban LCZs because the natural coverage is predominant over Europe (93,1%). In both cases, there are some cells with a negative spatial correlation. In the case of CLMS-IMD, there is an increase in the percentage of cells with a negative spatial correlation that has been further analysed in the following comparison C2.

Fig. 2 shows the spatial distribution of the ten urban LCZs provided by ECOCLIMAP-SG and their percentage over Europe. The LCZ9 "Sparsely built" is the predominant urban field, with a percentage higher than 70%, while LCZ10 "Heavy industry" is the least common field (0.26%).<sup>2</sup> European countries reveal the predominance of open and large arrangements of buildings. At the same time, the most compact and densely areas are mainly located within the major cities, such as capitals and metropolitan areas. Fig. 3 shows the ISA field ( $ISA > 0$ ) provided by GAIA (Fig. 3a), GAUD (Fig. 3b) and CLMS-IMD (Fig. 3c) at 300 m resolution and the percentage of ISA over the total number of impervious cells. The percentage is calculated considering a classification in 10 classes of ISA from 0 to 1. GAIA and GAUD look very similar to each other: the majority of cells have an ISA ranging from 0 to 0.1 (~30%), from 0.6 to 0.7 (~25%) and higher than 0.9 (~30%). In contrast, CLMS-IMD shows a prevalence of cells with impervious areas lower than 0.1 (~80%) and a reduced presence of cells with high values of ISA. The difference between the datasets with the ISA field is related to the type of information they provide. In GAIA and GAUD, impervious pixels are considered 100% sealed surfaces, resulting in overestimating impervious areas. At the same time, CLMS-IMD provides the percentage of imperviousness from 1 to 100 for each cell resulting in more accurate detection and representation of impervious areas.

The datasets are also compared by associating the mean value and standard deviation of ISA to each urban LCZ. Fig. 4 shows the association of LCZs with GAIA (Fig. 4a), GAUD (Fig. 4b) and CLMS-IMD (Fig. 4c) and the comparison with the range of impervious surface area defined by Stewart and Oke (2012) for each urban LCZ. GAUD and GAIA return similar results again: the mean value of ISA associated with each LCZ is outside the range defined by Stewart and Oke (2012), confirming their tendency to overestimate. CLMS-IMD is more consistent: the mean values associated with LCZ1, LCZ5, LCZ6, LCZ8 and LCZ9 are within the range, while in the other cases (LCZ2 and LCZ3), they are slightly larger than the upper value. LCZ10 is a particular case in all three comparisons: the mean value of ISA is about 80% for GAIA and GAUD and is equal to 60% for CLMS-IMD. In all cases, the mean values are higher than the upper values of the range.

<sup>1</sup> The Organisation for Economic Cooperation and Development (OECD) and the European Commission have jointly developed a methodology to provide a harmonised definition of FUAs across countries, overcoming limitations for international comparability of densely populated areas linked to administrative boundaries.

<sup>2</sup> LCZ4 "Open high-rise" and LCZ7 "Lightweight low-rise" are not available in the European map. The technical documentation does not provide further details.

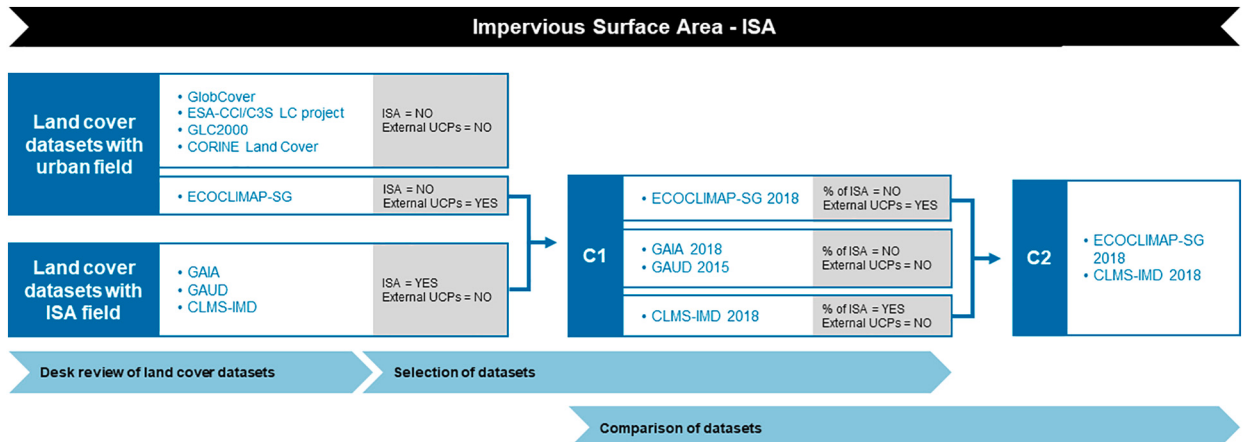


Fig. 1. Methodological workflow.

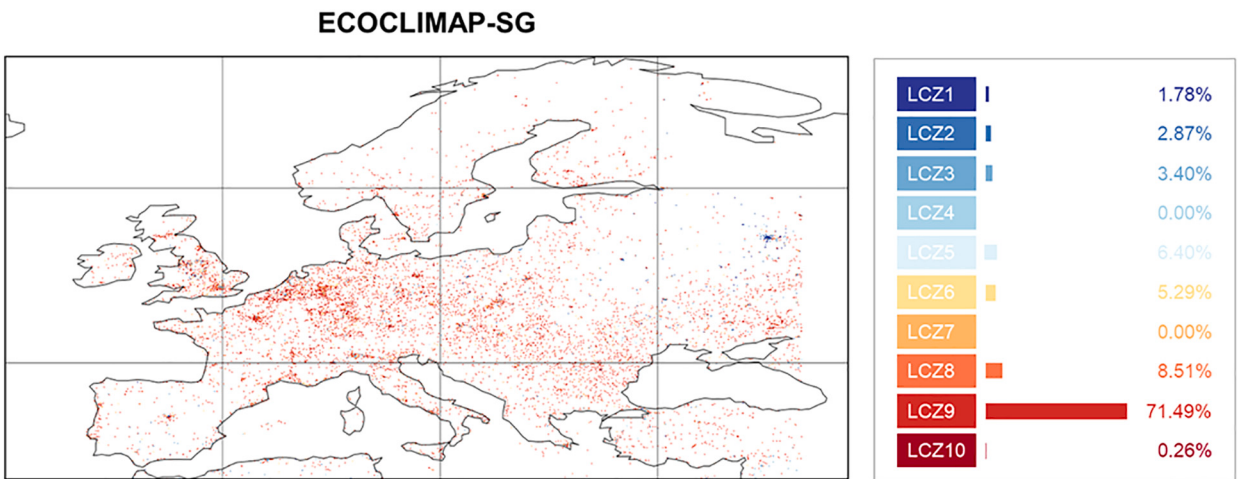


Fig. 2. Spatial distribution of urban LCZs provided by ECOCLIMAP-SG over Europe. The values on the right show the percentage of each LCZ over Europe.

As a result of this comparison, CLMS-IMD seems to be the most suitable dataset to represent ISA as it provides the percentage of imperviousness, and its values are more consistent with the impervious surface fraction as defined by [Stewart and Oke \(2012\)](#). For this reason, CLMS-IMD is selected for the following comparison with ECOCLIMAP-SG at the local level.

### 3.2. Comparison at the local level

The second comparison concerns the ISA provided by CLMS-IMD and the LCZs of ECOCLIMAP-SG. The datasets are compared at the local level for the three cities of Barcelona, Budapest and Milan. A spatial correlation analysis is also carried out in this case. [Table 4](#) shows a negative spatial correlation between the two datasets for the three cities, with many pixels represented oppositely. A large number of pixels is classified as natural in ECOCLIMAP-SG and impervious in CLMS-IMD, particularly in the case of Milan (17%). In comparison, the other cities show slightly lower values but are still relevant (11% for Barcelona and 8% for Budapest). A discordance also exists between urban LCZs and pervious cells, with values below 10% in all cases.

Furthermore, [Figs. 5, 6 and 7](#) show, respectively, the results for Barcelona, Budapest and Milan: the spatial distribution of ISA derived from the imperviousness density (1–100%) provided by CLMS-IMD resampled at 300 m (a), the ten urban LCZs provided by ECOCLIMAP-SG (b) and the association of ISA with LCZs represented as mean and standard deviation (c). Looking at the maps in the upper part of the figures, it is clear that there is a similarity in the spatial distribution of the impervious pixels and the cells identified as urban LCZ.

In the case of Barcelona, the graph ([Fig. 5c](#)) shows that the mean values of ISA are consistent with the ranges defined by [Stewart and Oke \(2012\)](#) in some cases, confirming the results displayed at the European level for LCZ1, LCZ3, LCZ5, LCZ6, LCZ9 and LCZ10 ([Fig. 4c](#)). However, the mean ISA values associated with LCZ2 and LCZ8 are higher than the upper value of the ranges.

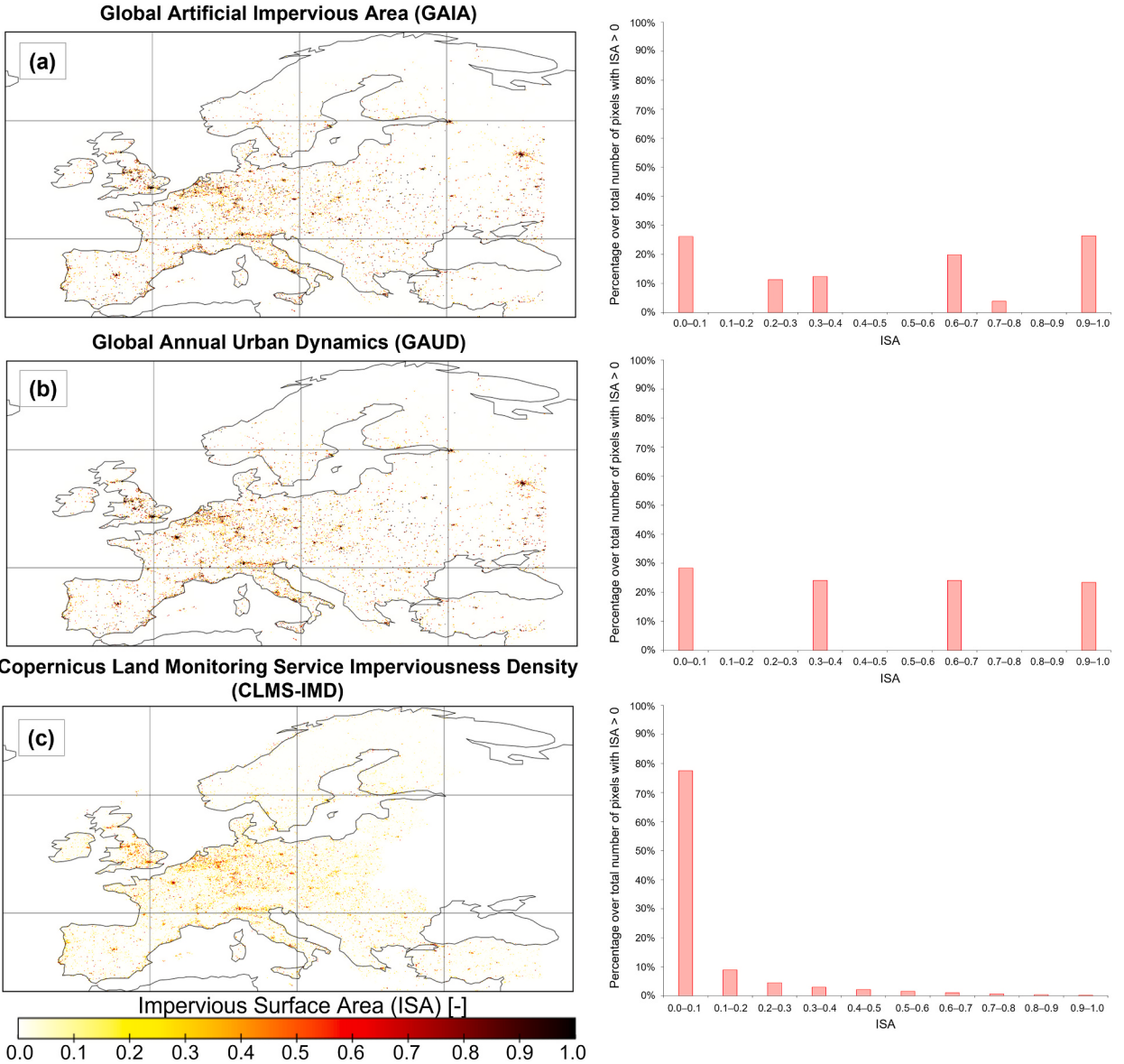


**Fig. 3.** Spatial distribution of ISA provided by (a) GAIA, (b) GAUD and (c) CLMS-IMD over Europe. The histograms on the right show the percentage of ISA over the total number of impervious cells. The percentage is calculated considering a classification in 10 classes of ISA from 0 to 1.

The situation is similar for the city of Budapest (Fig. 6c), except for the LCZ10, for which the mean value is equal to the upper value of the range. In the case of Milan (Fig. 7c), some differences with the European results are evident for LCZ1 and LCZ8, for which the mean values are higher than the upper values of the ranges defined by [Stewart and Oke \(2012\)](#). In this case, LCZ10 is missing. Thus it is not possible to make a comparison.

Such a comparison highlights a general overestimation of ISA by CLMS-IMD against the ranges defined by [Stewart and Oke \(2012\)](#), particularly evident in the case of LCZ2, LCZ8 and LCZ10.

A further comparison between CLMS-IMD and ECOCLIMAP-SG concerns the green areas. Two green areas located within the historical centres of each city are selected to verify how each dataset identifies them. Figs. 8, 9 and 10 show that the green areas and parks chosen for each city are mainly represented as pervious surface areas by CLMS-IMD, and as LCZ9 “Sparsely built” by ECOCLIMAP-SG. LCZ9 includes small or medium-sized buildings widely spaced across the landscape, with scattered trees and significant plant cover. A comparison with CLMS-IMD could be a suitable way to identify the actual impervious surface areas within the LCZ9, thus excluding the previous ones from the urban LCZs.

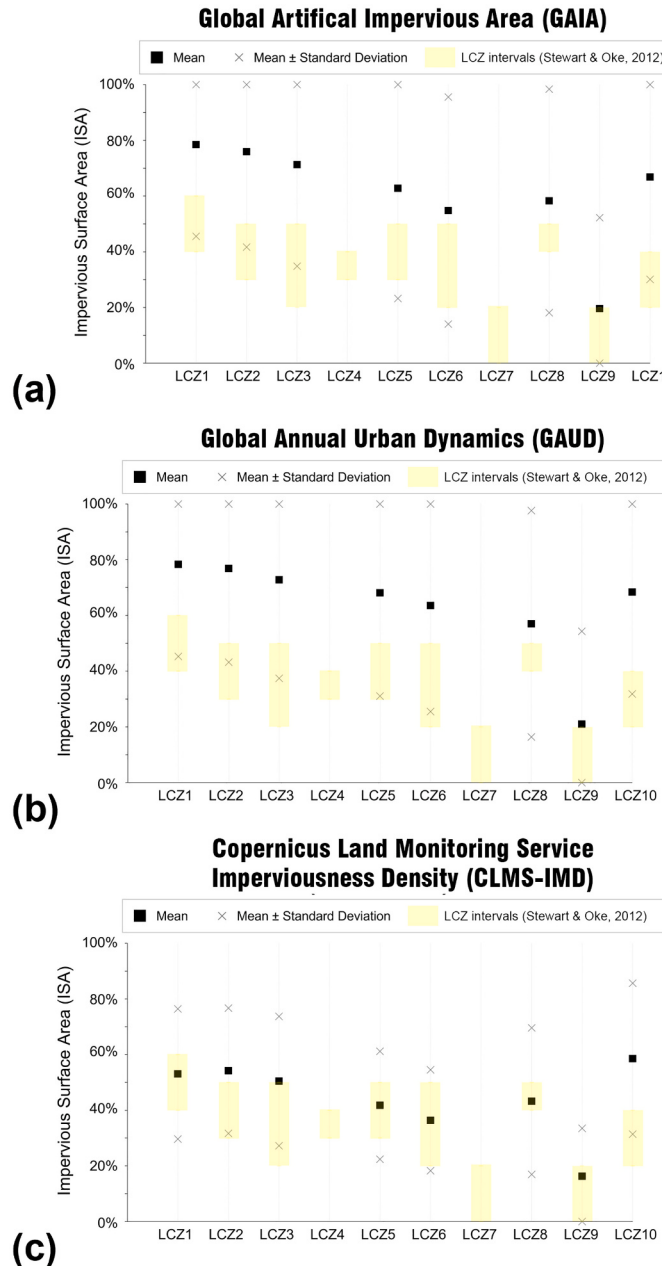


**Fig. 4.** Association of ISA provided by (a) GAIA, (b) GAUD and (c) CLMS-IMD with urban LCZs over Europe (LCZs are provided by ECOCLIMAP-SG).

#### 4. Conclusions, remarks and future developments

This study has investigated the ability of land cover datasets available for Europe to represent the impervious surface area by selecting datasets with different features and comparing them at both pan-European and local levels. The main findings of the comparison are:

1. Land cover datasets with urban fields (GlobCover, ESA CCI/C3S LC project, CORINE Land Cover) are not suitable to derive ISA because they also include (small) green areas in urban classes;
2. A land cover dataset with LCZs (ECOCLIMAP-SG), while not directly providing ISA values, includes several parameters that can be incorporated as input data in numerical atmospheric models, improving the urban parameterisation for very high-resolution climate and NWP modelling. For this reason, ECOCLIMAP-SG looks very promising for the aims of PP CITTÀ;

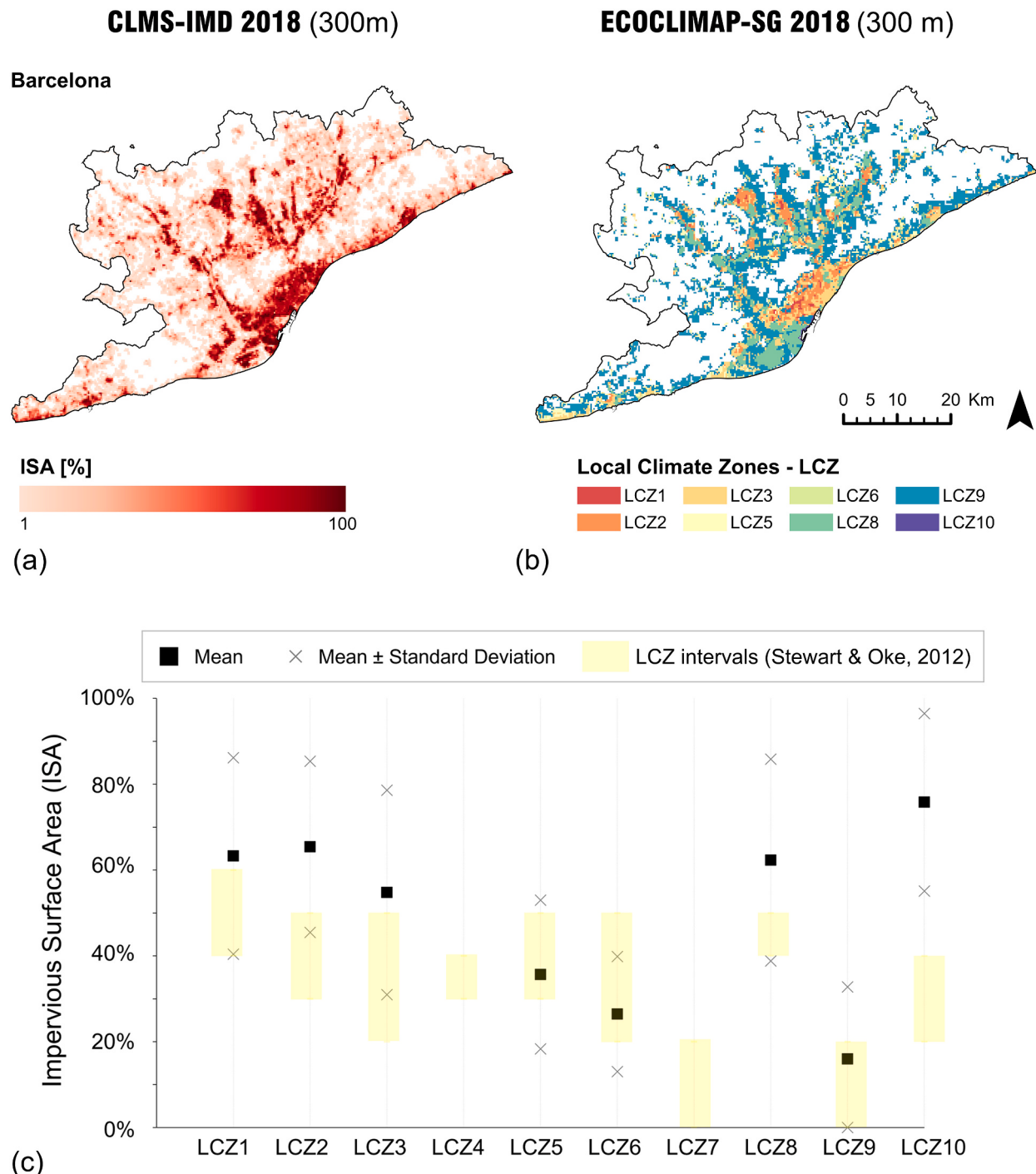


**Fig. 5.** Comparison between CLMS-IMD 2018 and ECOCLIMAP-SG for the city of Barcelona: spatial distribution of (a) ISA and (b) urban LCZs; (c) association of ISA with urban LCZs.

3. Land cover datasets with ISA field (GAIA, GAUD, CLMS-IMD) represent the impervious surface fraction more accurately with a clear distinction between impervious and pervious pixels. Their spatial resolution is a key factor in determining ISA;
4. The imperviousness degree provided by CLMS-IMD is consistent with the impervious surface fraction defined by [Stewart and Oke \(2012\)](#), although it is sometimes overestimated. Such an overestimation could affect the numerical simulations performed with ICON/TERRA\_URB. Quantifying whether the level of this inaccuracy is acceptable is difficult without performing ad hoc numerical simulations. In general, other recent and detailed datasets might be more suitable for estimating the values of ISA and other urban

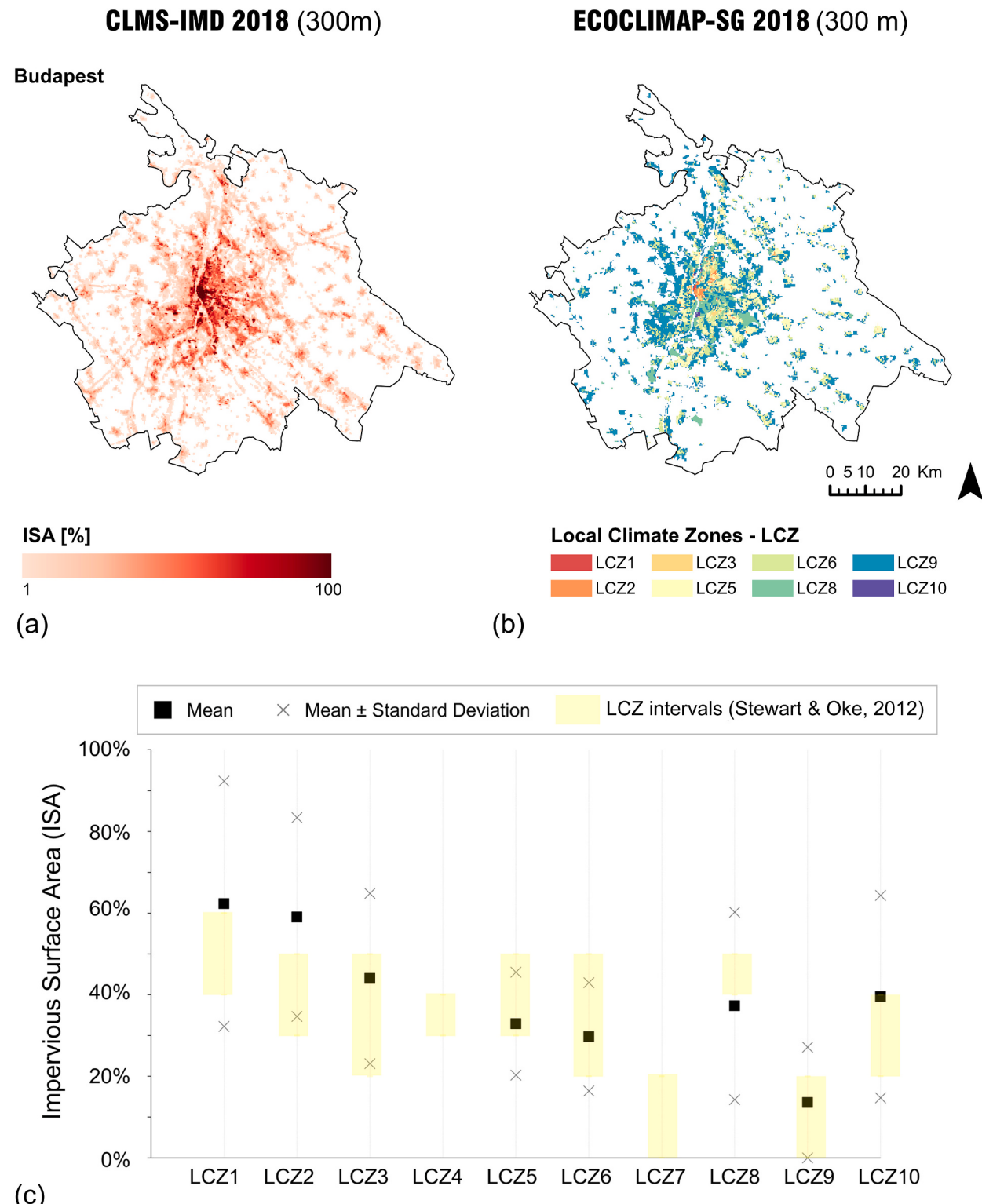


**Fig. 6.** Comparison between CLMS-IMD 2018 and ECOCLIMAP-SG for the city of Budapest: spatial distribution of (a) ISA and (b) urban LCZs; (c) association of ISA with urban LCZs.

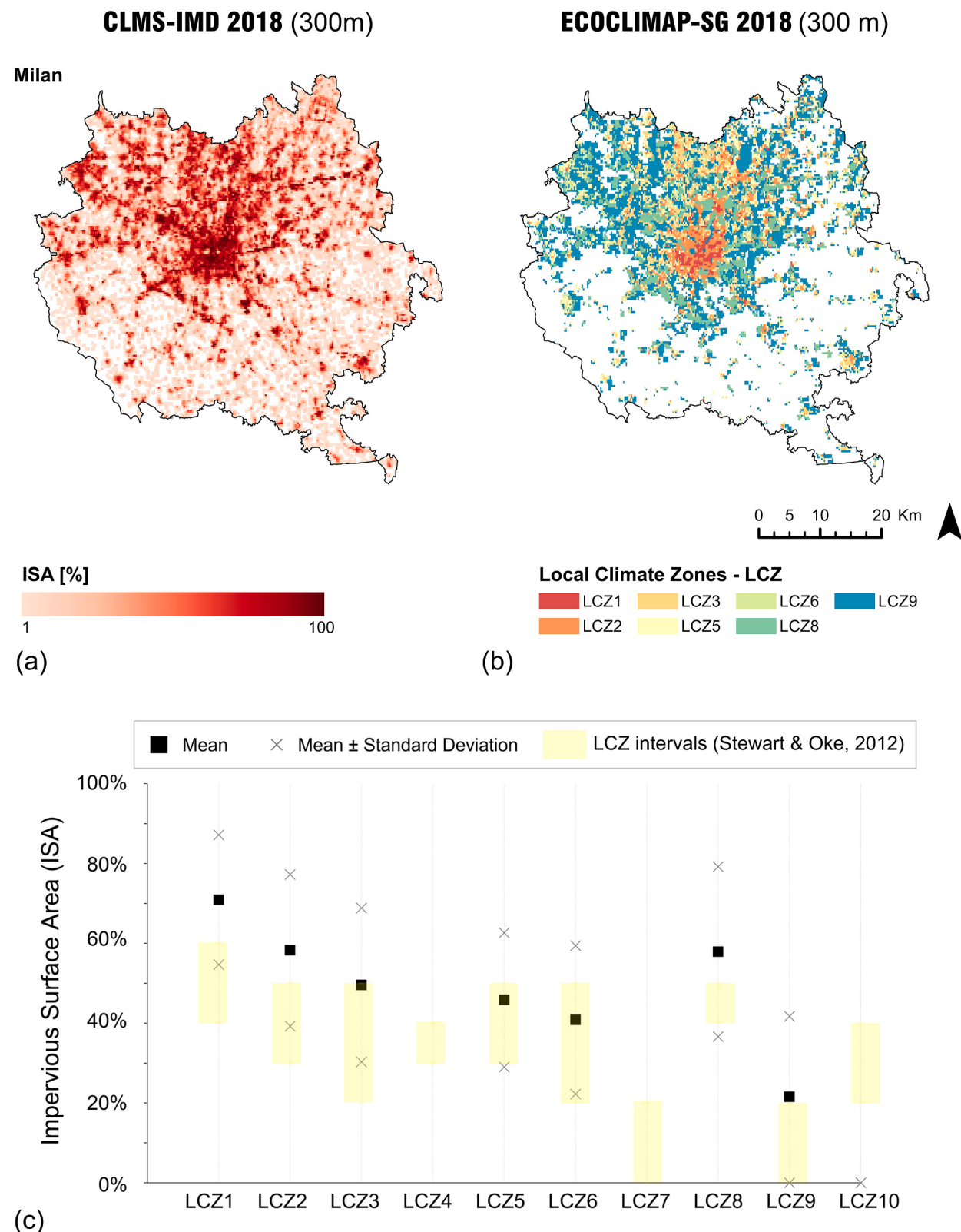


**Fig. 7.** Comparison between CLMS-IMD 2018 and ECOCLIMAP-SG for the city of Milan: spatial distribution of (a) ISA and (b) urban LCZs; (c) association of ISA with urban LCZs.

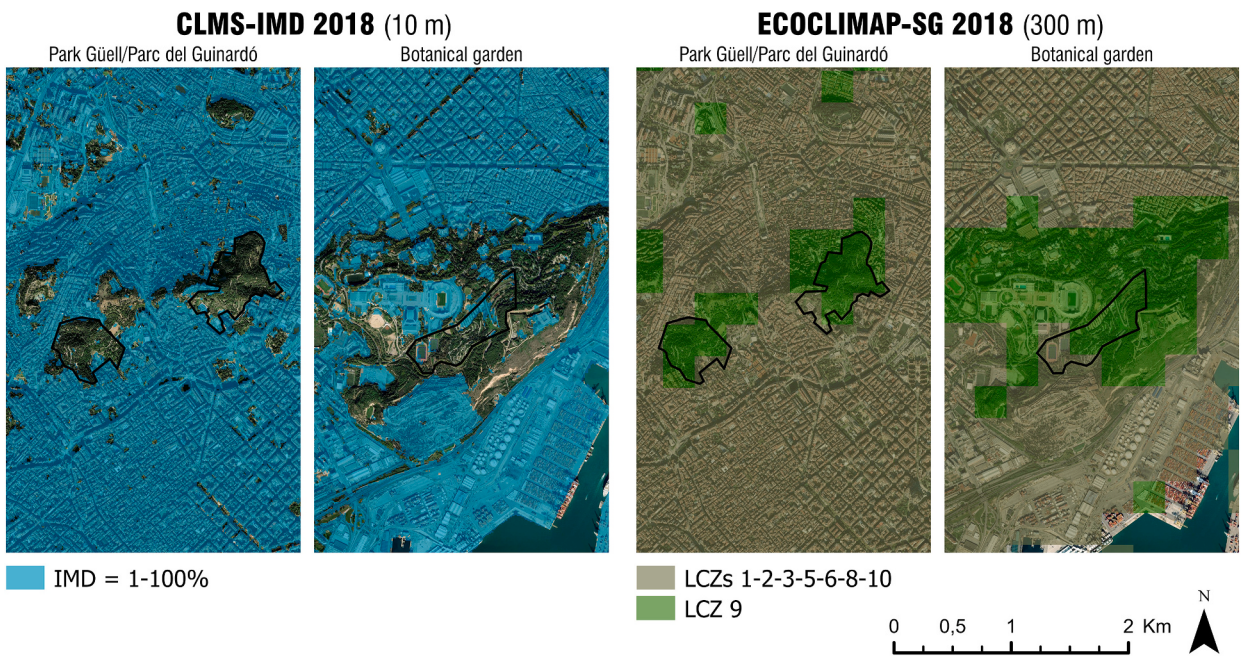


**Fig. 8.** Comparison between CLMS-IMD 2018 and ECOCLIMAP-SG for the city of Barcelona – green areas. (For interpretation of the references to colour in this figure legend, the reader is referred to the web version of this article.)

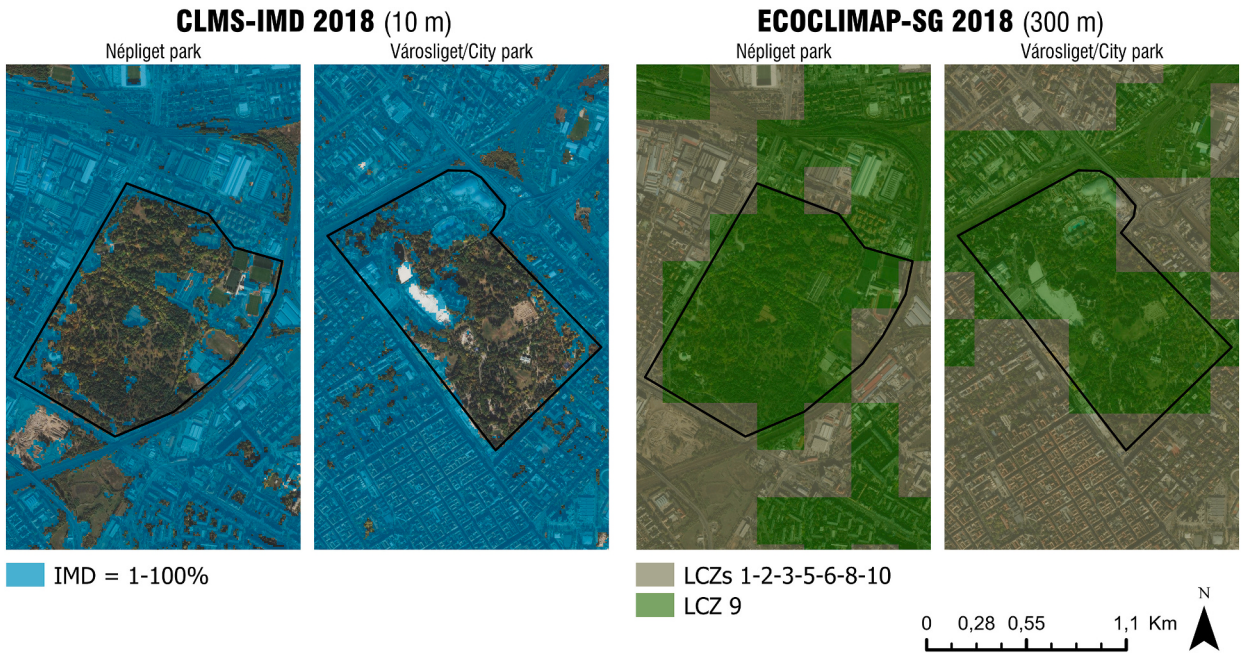


**Fig. 9.** Comparison between CLMS-IMD 2018 and ECOCLIMAP-SG for the city of Budapest – green areas. (For interpretation of the references to colour in this figure legend, the reader is referred to the web version of this article.)

properties. However, these datasets provide only one parameter, which needs to be harmonised before being integrated into TERRA-URB. [Stewart and Oke \(2012\)](#) were chosen as a reference for comparison because the LCZs include not only ISA but also all parameters associated with urban coverage. Despite the uncertainty that has to be considered, LCZs (and ECOCLIMAP-SG) are preferable to other datasets to achieve the objective of the study.

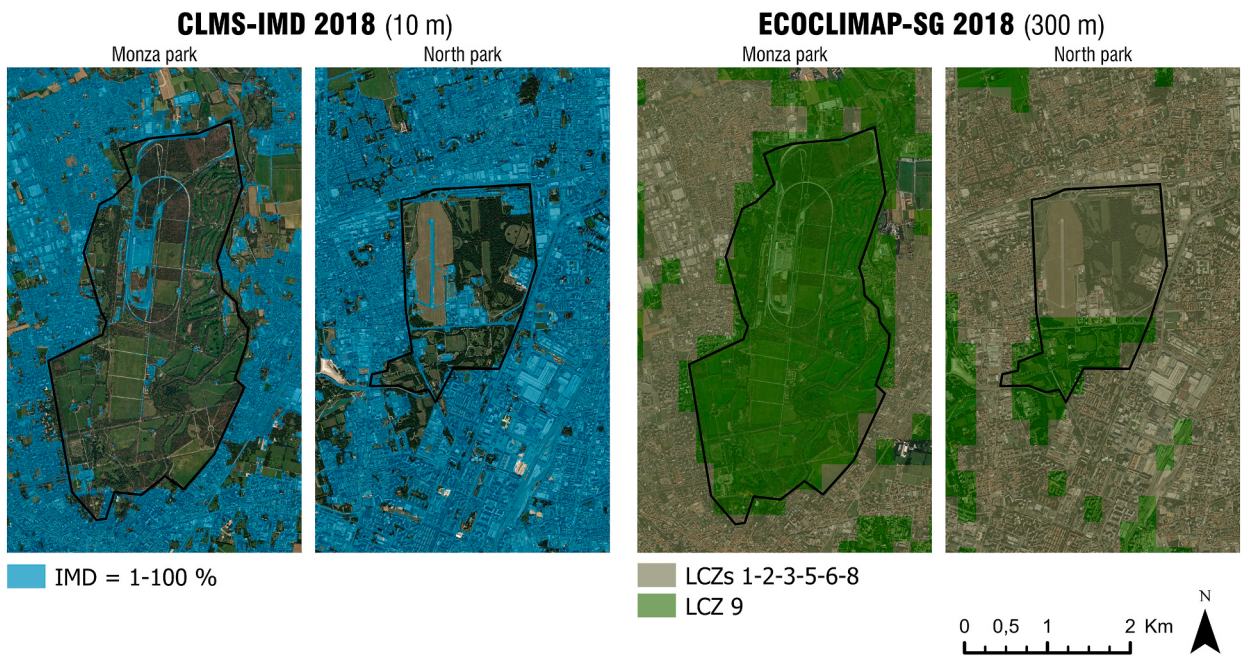


**Fig. 10.** Comparison between CLMS-IMD 2018 and ECOCLIMAP-SG for the city of Milan – green areas. (For interpretation of the references to colour in this figure legend, the reader is referred to the web version of this article.)

The relevance of this work is related to the presence of a constantly evolving land cover in urban areas that requires a detailed and dynamic representation over time and space. According to the need for high-resolution atmospheric simulations in cities, adopting a dataset that includes information on all artificially sealed areas and capturing the percentage and change of soil sealing over time and space is essential to properly describe the impacts of land cover on weather and climate. Another key issue concerns the derivation of high-resolution and dynamic external parameters consistent with the ISA values.

In this perspective, a workflow is proposed to harmonise ISA and external UCPs based on the CLMS-IMD and ECOCLIMAP-SG datasets. The workflow is structured as follows (Fig. 11):

- **Step 1: Data collection for ISA and external UCPs.** The required data come from Pan-European datasets. This information includes the percentages of impervious coverage provided by CLMS-IMD at 10 m for 2018 and the presence of urban LCZs, derived from ECOCLIMAP-SG at 300 m, with the associated UCPs that could be adopted as external parameters.
- **Step 2: Interpolation of ISA on urban LCZ.** In this step, ISA values are remapped by adopting the same grid and spatial resolution of ECOCLIMAP-SG to analyse, in the next step, the spatial relationship with urban LCZs.
- **Step 3: Correlation of ISA values with LCZ.** This step consists of the association of the mean ISA values (1–100%) with urban LCZs to identify a variability range of ISA for each LCZ, which is then compared with the corresponding range defined in [Stewart and Oke \(2012\)](#) for the impervious surface fraction.
- **Step 4: Harmonisation of ISA and datasets with external UCPs.** The correlation above allows the association of ISA with the external parameters derived from LCZs, thus avoiding inconsistencies and harmonising datasets.

The workflow mentioned above is adopted to identify the UCPs for the urban tile when TERRA-URB is activated. Instead, the external parameters associated with the natural tile, based on TERRA-ML, must be recalculated as an area-weighted average over the land cover classes, excluding the urban class.

The approach adopted in this study represents an advancement upon previous efforts in analysing and comparing land cover datasets with different features. It contributes to deepening the knowledge of the characteristics of each dataset and defining a process to derive consistent input data for high-resolution urban simulations. However, expanding the analysis to further case studies is particularly important to verify the results obtained in this study. Future work could focus on comparing ECOCLIMAP-SG and CLMS-IMD and performing numerical experiments in the domains identified within the PP CITTÀ (i.e., Turin, Naples, Bucharest, Jerusalem and Tel Aviv, Warsaw) framework as well as in other cities in Europe and worldwide.

#### CRediT authorship contribution statement

**Carmela Apreda:** Methodology, Conceptualization, Software, Validation, Writing – original draft. **Jan-Peter Schulz:** Conceptualization, Writing – review & editing, Supervision. **Alfredo Reder:** Conceptualization, Methodology, Writing – review & editing,

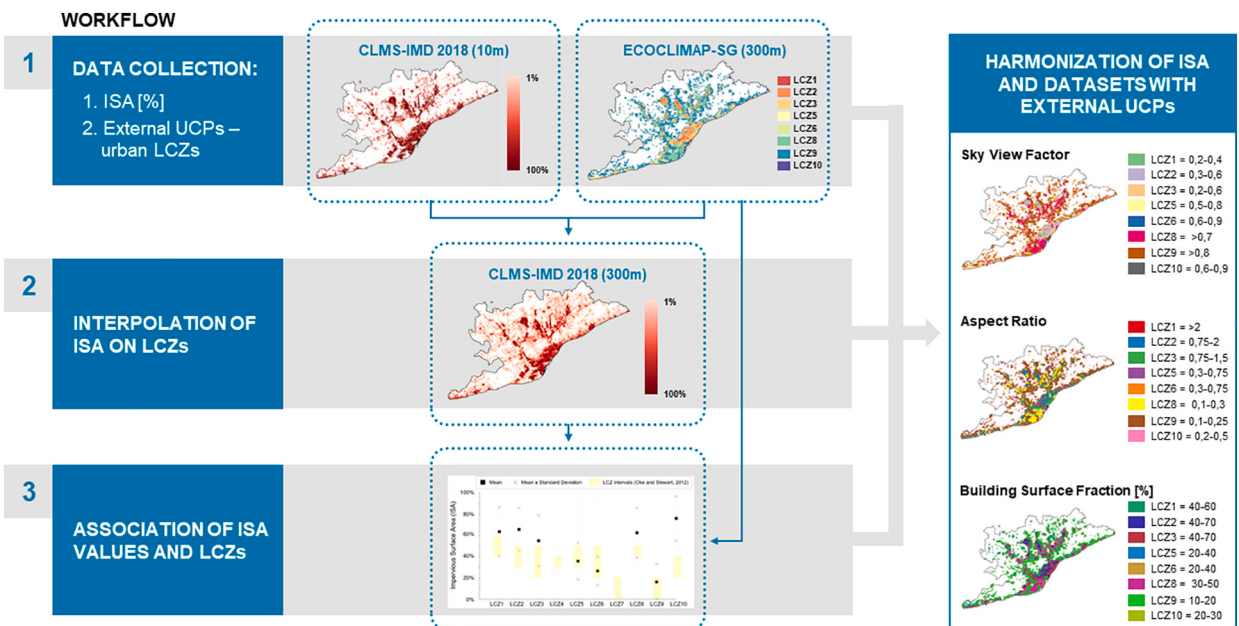


Fig. 11. Workflow to harmonise ISA and external UCPs.

Investigation, Validation. Paola Mercogliano: Conceptualization, Writing – review & editing, Supervision.

#### Declaration of competing interest

The authors declare that they have no known competing financial interests or personal relationships that could have appeared to influence the work reported in this paper.

#### Data availability

Data will be made available on request.

#### Acknowledgements

The study is carried out within the COSMO Priority Project CITTÀ aimed at developing the urban module in ICON(-LAM). We would like to thank Francesco Repola and Carmine De Lucia (CMCC) for supporting us. Further information can be found at: <https://bit.ly/3H4qwAF>.

#### References

- Adinolfi, M., Raffa, M., Reder, A., Mercogliano, P., 2021. Evaluation and expected changes of summer precipitation at convection permitting scale with COSMO-CLM over alpine space. *Atmosphere* 12, 54. <https://doi.org/10.3390/atmos12010054>.
- Arino, O., Perez, J.R., Kalogirou, V., Defourny, P., Achard, F., 2009. GlobCover 2009. European Space Agency, Paris.
- Baldauf, M., Seifert, A., Förstner, J., Majewski, D., Raschendorfer, M., Reinhardt, T., 2011. Operational convective-scale numerical weather prediction with the COSMO model: description and sensitivities. *Mon. Weather Rev.* 139, 3887–3905. <https://doi.org/10.1175/mwr-d-10-05013.1>.
- Ban, N., et al., 2021. The first multi-model ensemble of regional climate simulations at kilometer-scale resolution, part I: evaluation of precipitation. *Clim. Dyn.* 57, 275–302. <https://doi.org/10.1007/s00382-021-05708-w>.
- Ban, N., Schmidli, J., Schär, C., 2014. Evaluation of the new convective-resolving regional climate modelling approach in decade-long simulations. *J. Geophys. Res. Atmos.* 119, 7889–7907. <https://doi.org/10.1002/2014JD021478>.
- Bartholomé, E., Belward, A., 2005. GLC 2000, a new approach to global land cover mapping from earth observation data. *Int. J. Remote Sens.* 26 (9), 1959–1977. <https://doi.org/10.1080/0143116041233129129>.
- Berthou, S., Kendon, E.J., Chan, S.C., Ban, N., Leutwyler, D., Schar, C., Fosser, G., 2018. Pan-European climate at convection-permitting scale: a model intercomparison study. *Clim. Dyn.* 5, 1–25. <https://doi.org/10.1007/s00382-018-4114-6>.
- Bontemps, S., Defourny, P., Van Bogaert, E., Arino, O., Kalogirou, V., Ramos Perez, J., 2011. GLOBCOVER 2009. Products description and validation report. UCLouvain & ESA team. Available at. <https://bit.ly/3KRkmGe>. Accessed 03/12/2021.
- Bukovsky, M.S., Gao, J., Mearns, L.O., O'Neill, B.C., 2021. SSP-based land-use change scenarios: a critical uncertainty in future regional climate change projections. *Earth's Future* 9 (3). <https://doi.org/10.1029/2020EF001782> e2020EF001782.
- Büttner, G., Kosztra, B., Maucha, G., Pataki, R., Kleeschulte, S., Hazeu, G., Vittek, M., Schröder, C., Littkopp, A., 2021. Copernicus land monitoring service, CORINE land cover, user manual. European Union, Copernicus land monitoring service 2021, European Environment Agency (EEA). Available at. <https://bit.ly/3pRp26D>. Accessed 03/12/2021.
- CNRM, 2018a. ECOCLIMAP-Second Generation. Available at: <https://bit.ly/3HjQHoW>. Accessed 03/12/2021.

- CNRM, 2018b. ECOCLIMAP-SG: technical documentation. Available at: <https://bit.ly/3mMcZGg>. Accessed 03/12/2021.
- Coffey, R., 2013, January 18. The Difference between “Land Use” and “Land Cover”. Michigan State University Extension. [https://www.canr.msu.edu/news/the\\_difference\\_between\\_land\\_use\\_and\\_land\\_cover](https://www.canr.msu.edu/news/the_difference_between_land_use_and_land_cover).
- Coppola, E., Sobolowski, S., Pichelli, E., et al., 2020. A first-of-its-kind multi-model convection permitting ensemble for investigating convective phenomena over Europe and the Mediterranean. *Clim. Dyn.* 55, 3–34. <https://doi.org/10.1007/s00382-018-4521-8>.
- Davin, E.L., Rechid, D., Breil, M., Cardoso, R.M., Coppola, E., Hoffmann, P., Jach, L., Katragkou, E., de Noblet-Ducoudré, N., Radtke, K., Raffa, M., Soares, P.M., Sofiadis, G., Strada, S., Strandberg, G., Tölle, M.H., Warrach-Sagi, K., Wulfmeyer, V., 2020. Biogeophysical impacts of forestation in Europe: first results from the LUCAS (land use and climate across scales) regional climate model intercomparison. *Earth System Dynamics* 11, 183–200. <https://doi.org/10.5194/esd-11-183-2020>.
- Defourny, P., Lamarche, C., Bontemps, S., De Maet, T., Van Bogaert, E., Moreau, I., Brockmann, C., Boettcher, M., Kirches, G., Wevers, J., Santoro, M., Ramoino, F., Arino, O., 2017. Land cover climate change initiative - product user guide v2. Issue 2.0. Available at: <https://bit.ly/3xTGUB9>. Accessed 03/12/2021.
- Defourny, P., Lamarche, C., Marissiaux, Q., Carsten, B., Martin, B., Grit, K., 2021. *Product user guide and specification - ICDR land cover 2016-2020*, version 1.1. Available at: <https://bit.ly/32XkzHD>. Accessed 03/12/2021.
- Di Gregorio, A., Jansen, L.J.M., 2000. Land cover classification system (LCCS): classification concepts and user manual. Food and agriculture Organization of the United Nations, Rome. Available at: <https://bit.ly/3GjAbDO>. Accessed 03/12/2021.
- Dijkstra, L., Poelman, H., 2012. Cities in Europe. In: *The new OECD-EC definition*. RF 1/2012. Available at: <https://bit.ly/3sQRG9m>. Accessed 03/02/2022.
- EEA, 2004. EEA Glossary. Available at: <https://bit.ly/3HkvRWD>. Accessed 03/12/2021.
- EEA, 2018. CORINE Land Cover. Available at: <https://bit.ly/3n1BFLn>. Accessed 03/12/2021.
- EEA, 2020a. Imperviousness Density 2018. Available at: <https://bit.ly/3xsqVKu>. Accessed 03/12/2021.
- EEA, 2020b. *HRL Imperviousness Degree 2018 Validation Report*. GMES Initial Operations / Copernicus Land monitoring services – Validation of products, Validation Services for the geospatial products of the Copernicus land Continental and local components including in-situ data (lot 1), Open Call for Tenders - EEA/MDI/14/010, Fourth Specific Contract - No 3436/R0-COPERNICUS/EEA.57889. Available at: <https://bit.ly/3qYAFu3>. Accessed 03/12/2021.
- ESA & UCLouvain, 2010. GlobCover. Available at: [http://due.esrin.esa.int/page\\_globcover.php](http://due.esrin.esa.int/page_globcover.php). Accessed 03/12/2021.
- ESA-CCI, 2022. Land Cover Classification Gridded Maps from 1992 to Present Derived from Satellite Observations. Available at: <https://bit.ly/3txoNAi>. Accessed 03/01/2022.
- EU-JRC, 2003. Global Land Cover 2000 - Products. Available at: <https://bit.ly/3tAPpQS>. Accessed 03/12/2021.
- Flanner, G., 2009. Integrating anthropogenic heat flux with global climate models. *Geophys. Res. Lett.* 36, L02801. <https://doi.org/10.1029/2008GL036465>.
- Fosser, G., Khodayar, S., Berg, P., 2015. Benefit of convection permitting climate model simulations in the representation of convective precipitation. *Clim. Dynam.* 44 (1–2), 45–60. <https://doi.org/10.1007/s00382-014-2242-1>.
- Fowler, H.J., Wasko, C., Prein, A.F., 2021. Intensification of short-duration rainfall extremes and implications for flood risk: current state of the art and future directions. *Phil. Trans. R. Soc. A* 379, 2019054. <https://doi.org/10.1098/rsta.2019.0541>.
- Fumiére, Q., Déqué, M., Nuissier, O., Somot, S., Alias, A., Caillaud, C., Laurantin, O., Seity, Y., 2020. Extreme rainfall in Mediterranean France during the fall: added-value of the CNRM-AROME convection permitting regional climate model. *Clim. Dyn.* 55, 77–91. <https://doi.org/10.1007/s00382-019-04898-8>.
- GCOS, 2023. Essential climate variables. Available at: <https://gcos.wmo.int/en/essential-climate-variables>. Accessed 03/12/2021.
- Gong, P., Li, X., Wang, J., Bai, Y., Chen, B., Hu, T., Liu, X., Xu, B., Yang, J., Zhang, W., Zhou, Y., 2019. GAIA file list. Available at: <https://bit.ly/3bhABxb>. Accessed 03/12/2021.
- Gong, P., Li, X., Wang, J., Bai, Y., Chen, B., Hu, T., Liu, X., Xu, B., Yang, J., Zhang, W., Zhou, Y., 2020. Annual maps of global artificial impervious area (GAIA) between 1985 and 2018. *Remote Sens. Environ.* 236, 111510 <https://doi.org/10.1016/j.rse.2019.111510>.
- Huang, Y., 2020. High spatiotemporal resolution mapping of global urban change from 1985 to 2015. Available at: <https://doi.org/10.6084/m9.figshare.11513178.v1>. Accessed 03/12/2021.
- IPCC, 2022. Sixth assessment report. In: Intergovernmental panel on climate change. Available at: <https://bit.ly/3zB8WUT>. Accessed 03/06/2022 [accepted version subject to final edits].
- Kosztra, B., Büttner, G., Hazeu, G., Arnold, S., 2019. Updated CLC illustrated nomenclature guidelines. In: European topic Centre on urban, land and soil systems (ETC/ULS). Available at: <https://bit.ly/3oD6Fmj>. Accessed 03/12/2021.
- Le Moigne, P., et al., 2018. SURFEX Scientific Documentation. Available at: [https://www.umr-cnrm.fr/surfex/IMG/pdf/surfex\\_scidoc\\_v8.1.pdf](https://www.umr-cnrm.fr/surfex/IMG/pdf/surfex_scidoc_v8.1.pdf). Accessed 15/03/2023.
- Lin, Y.Z., Liu, A.P., Ma, E.J., Li, X., Shi, Q.L., 2013. Impacts of future urban expansion on regional climate in the northeast megalopolis, USA. *Adv. Meteorol.* 2013, 362925 <https://doi.org/10.1155/2013/362925>.
- Liu, X., Huang, Y., Xu, X., Li, X., Ciais, P., Lin, P., Gong, K., Ziegler, A.D., Chen, A., Gong, P., Chen, J., Hu, G., Chen, Y., Wang, S., Wu, Q., Huang, K., Estes, L., Zeng, Z., 2020. High-spatiotemporal-resolution mapping of global urban change from 1985 to 2015. *Nature Sustainab.* 3, 564–570. <https://doi.org/10.1038/s41893-020-0521-x>.
- Maucha, G., Büttner, G., Kosztra, B., 2010. European Validation of GMES FTS Soil Sealing Enhancement. Final draft. European Environment Agency, European Topic Centre Land Use and Spatial Information.
- Piazza, M., Prein, A., Truhetz, H., Csaki, A., 2019. On the sensitivity of precipitation in convection-permitting climate simulations in the eastern alpine region. *Meteorol. Z.* 28 (4), 323–346. <https://doi.org/10.1127/metz/2019/0941>.
- Prein, A.F., Langhans, W., Fosser, G., Ferrone, A., Ban, N., Goergen, K., et al., 2015. A review on regional convection-permitting climate modeling: demonstrations, prospects, and challenges. *Rev. Geophys.* 53 (2), 323–361. <https://doi.org/10.1002/2014RG000475>.
- Raffa, M., Reder, A., Marras, G.F., Mancini, M., Scipione, G., Santini, M., Mercogliano, P., 2021. VHR-REA\_IT dataset: very high resolution dynamical downscaling of ERA5 reanalysis over Italy by COSMO-CLM. *Data* 6, 88. <https://doi.org/10.3390/data6080088>.
- Reder, A., Raffa, M., Montesarchio, M., Mercogliano, P., 2020. Performance evaluation of regional climate model simulations at different spatial and temporal scales over the complex orography area of the alpine region. *Nat. Hazards* 102, 151–177. <https://doi.org/10.1007/s11069-020-03916-x>.
- Reder, A., Raffa, M., Padulano, R., Rianna, G., Mercogliano, P., 2022. Characterising extreme values of precipitation at very high resolution: an experiment over twenty European cities. *Weather Clim. Extr.* 35, 100407 <https://doi.org/10.1016/j.wace.2022.100407>.
- Schulz, J.-P., Vogel, G., 2020. Improving the processes in the land surface scheme TERRA: bare soil evaporation and skin temperature. *Atmosphere* 11, 513. <https://doi.org/10.3390/atmos11050513>.
- Schulz, J.-P., Vogel, G., Becker, C., Kothe, S., Rummel, U., Ahrens, B., 2016. Evaluation of the ground heat flux simulated by a multi-layer land surface scheme using high-quality observations at grass land and bare soil. *Meteorol. Z.* 25, 607–620. <https://doi.org/10.1127/metz/2016/0537>.
- Shepherd, J.M., Carter, M., Manyin, M., Messen, D., Burian, S., 2010. The impact of urbanization on current and future coastal precipitation: a case study for Houston. *Environ. Plann. B: Plann. Des.* 37 (2), 284–304. <https://doi.org/10.1068/b34102t>.
- Sleeter, B.M., Loveland, T., Domke, G., Herold, N., Wickham, J., Wood, N., 2018. In: Reidmiller, D.R., Avery, C.W., Easterling, D.R., Kunkel, K.E., Lewis, K.L.M., Maycock, T.K., Stewart, B.C. (Eds.), Land Cover and Land-Use Change. In Impacts, Risks, and Adaptation in the United States: Fourth National Climate Assessment, U.S. Global Change Research Program, Washington, DC, USA, Volume II, pp. 202–231. <https://doi.org/10.7930/NCA4.2018.CH5>.
- Stewart, I.D., 2011. Redefining the Urban Heat Island. Doctoral dissertation. University of British Columbia, Vancouver. Retrieved June 10, 2022, from: <https://open.library.ubc.ca/collections/ubctheses/24/items/1.0072360>.
- Stewart, I.D., Oke, T.R., 2012. Local climate zones for urban temperature studies. *Bull. Am. Meteorol. Soc.* 93 (12), 1879–1900. <https://doi.org/10.1175/BAMS-D-11-00019.1>.
- Tsendbazar, N.E., de Bruin, S., Herold, M., 2015. Assessing global land cover reference datasets for different user communities. *ISPRS J. Photogramm. Remote Sens.* 103, 93–114. <https://doi.org/10.1016/j.isprsjprs.2014.02.008>.

- Verburg, P.H., Neumann, K., Nol, L., 2011. Challenges in using land use and land cover data for global change studies. *Glob. Chang. Biol.* 17, 974–989. <https://doi.org/10.1111/j.1365-2486.2010.02307.x>.
- Wouters, H., Varentsov, M., Blahak, U., Schulz, J.-P., Schättler, U., Buccignani, E., Demuzere, M. (2017). User Guide for TERRA.URB v2.2: the Urban-Canopy Land-Surface Scheme of the COSMO Model. doi:[10.13140/RG.2.2.33691.87847/1](https://doi.org/10.13140/RG.2.2.33691.87847/1).
- Zängl, G., Reinert, D., Ripodas, P., Baldauf, M., 2015. The ICON (ICOsahedral non-hydrostatic) modelling framework of DWD and MPI-M: description of the non-hydrostatic dynamical core. *Q. J. R. Meteorol. Soc.* 141, 563–579.
- Zhang, M., Tölle, M., Hartmann, E., Xoplaki, E., Luterbacher, J., 2021. A sensitivity assessment of COSMO-CLM to different land cover schemes in convection-permitting climate simulations over Europe. *Atmosphere* 12, 1595. <https://doi.org/10.3390/atmos12121595>.